NURETH14-384

GEOMETRIC EFFECTS OF 90-DEGREE VERTICAL ELBOWS ON GLOBAL TWO-PHASE FLOW PARAMETERS

M. Yadav, and S. Kim
The Pennsylvania State University, State College, USA

Abstract

Geometric effects of 90-degree vertical elbows on global two-phase flow parameters, in particular pressure drop and flow regime transition are investigated. Pressure measurements are obtained along the test section over a wide range of flow conditions in both single-phase and two-phase flow conditions. A two-phase pressure drop correlation analogous to Lockhart-Martinelli correlation is proposed to predict the minor loss across the elbows. Flow visualization is performed to study the effect of elbows on the two-phase flow regime transition. Modified flow regime maps for horizontal and vertical-downward two-phase flow are obtained which demonstrate that downstream of the elbows flow regime transition boundaries deviate significantly from the conventional flow regime transition boundaries.

Introduction

Most energy systems including the nuclear reactors have fluid flow channels in varying orientation and interconnected via flow restrictions. These flow restrictions have a significant effect on the transport of two-phase flow parameters and bubble interaction mechanisms which can lead to flow regime transition. The mass, momentum and energy transfer of any two-phase flow are greatly influenced by the interfacial structures and their transport characteristics. Hence, an experimental study is crucial in improving the understanding of effects of flow restrictions on two-phase flow parameters and development of dynamic modeling of interfacial area concentration.

To analyze the two-phase flow at a basic level, it is necessary to classify different patterns of phase distribution that are specifically similar for different pipe sizes and fluid properties. Most of the studies on two-phase flow in past focused only on vertical or horizontal flow configurations. Among the limited studies on the effect of flow restrictions, Salcudean et al [1, 2] and Wang et al [3] demonstrated the effect of various sizes and shapes of flow obstructions on two-phase pressure drop and flow regime transition. Hwang et al [4] presented experimental and analytical studies on the phase separation in dividing T- and Y-junctions. Efforts have been directed towards the effect of elbows on two-phase pressure drop. Chenoweth and Martin [5] showed that the two-phase pressure drop across bends is higher than for the single-phase flow, but it can be correlated using the Lockhart-Martinelli model, originally developed for the straight pipes. Spedding et al [6] reported the two-phase pressure drop data for a 90-degree elbow connecting vertical-upward to horizontal flow channel. In a recent study, Kim et al [7] presented two-phase pressure drop data for a 90degree and 45-degree horizontal elbows and developed a new correlation analogous to the conventional Lockhart and Martinelli correlation in order to predict two-phase pressure drop across the elbows. The current study addresses the major effects of a 90-degree vertical elbow connecting vertical upward-to-horizontal section. The effects include the additional pressure drop due to minor losses in the elbow region and deviation of the flow regime transition boundaries from the conventional boundaries suggested for fully developed horizontal two-phase flow.

1. Experimental Facility

The experimental facility consists of both vertical-horizontal test sections made out of 50.8 mm inner diameter acrylic pipes connected by 90-degree vertical glass elbows. The elbow connecting vertical-upward to horizontal section and horizontal to vertical downward section will be referred to as vertical-upward elbow and vertical-downward elbow, respectively. A schematic of the test facility is shown in Fig. 1. The lengths of vertical and horizontal sections are 3.35m and 9.45m, yielding development lengths of 66 and 186 diameters, respectively. The facility is designed such that all the conceivable vertical-to-horizontal and horizontal-to-vertical flow configurations can be achieved by simple manipulation of valves to change the flow direction. As such vertical-upward or vertical-downward two-phase flow can be introduced via injection system A or injection system B in Fig. 1, respectively. In the present study, injection A is utilized to provide vertical-upward two-phase flow conditions at the inlet, and injector B serves as an exit. The two-phase injection system is designed to provide approximately uniform bubble size at the inlet for all flow conditions.

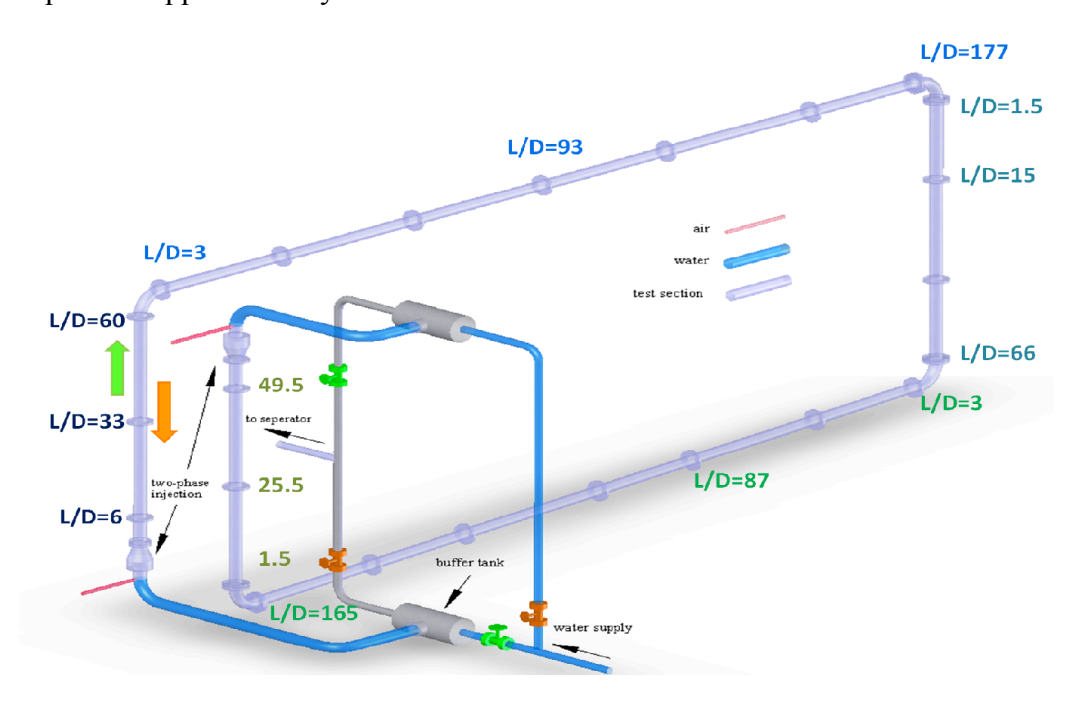


Figure 1 Simplified schematic diagram of combinatorial two-phase flow facility.

Filtered and de-ionized water is supplied to the test section from a 600 gallon accumulator tank by a 60 HP centrifugal pump. An air compressor supplies dry air at a pressure of 80 psig to an air accumulator. A magnetic flowmeter and rotameters measure the water flow rate and a set of air-rotameters control the gas flow rate. The magnetic flow meter has an accuracy of $\pm 0.5\%$ of the flow rate while the water and air rotameters have an accuracy of $\pm 2\%$ and $\pm 3\%$ of the full scale reading, respectively. At the exit of the loop, before water returns to the accumulator, a two-stage damper-separator system is installed to reduce the inertia of the flow and to break up any large gas pockets.

2. Results and Discussion

The experiments are performed at temperature, 25 °C, and atmospheric pressure. The results are divided into effect of elbows on the pressure drop and flow regime transition. A differential pressure transducer with an accuracy of \pm 1% of the reading is used to measure pressure and a high speed camera is employed to perform flow visualization study at measurement locations along the test section as shown in Fig. 2. The measurement ports are designed to facilitate pressure measurement, local conductivity probes, optical and flow visualization instrumentation. Each measurement port is made from a solid acrylic rod with part of the outer surface machined flat to minimize optical distortion and provide an ideal condition for both flow visualization and the optical instrumentation application.

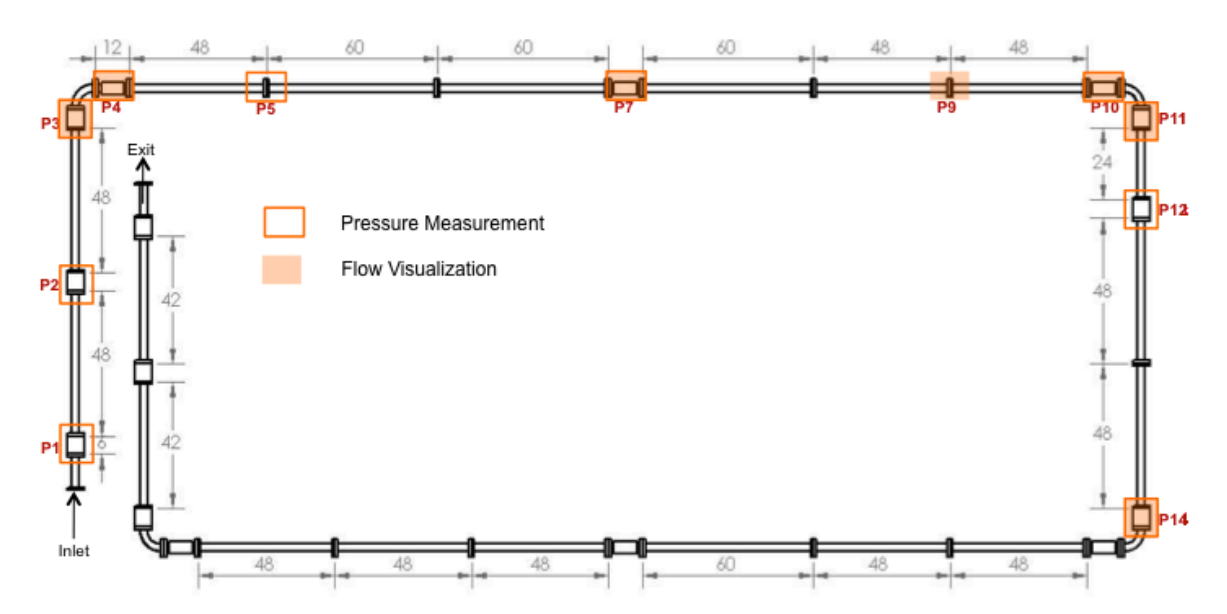


Figure 2 Simplified schematic of combinatorial two-phase flow facility showing the measurement locations.

2.1. Single-phase pressure

Differential pressure is measured for four single-phase liquid flow conditions at nine axial locations along the test section. The measurement locations in the vertical-upward section include ports P1, P2 and P3 located 6D, 33D and 60D downstream of the inlet respectively. In the horizontal section the measurements are obtained at ports P4, P7 and P10 located 3D, 93D and 177D downstream of the vertical upward elbow respectively. In the vertical downward section measurement locations include ports P11, P12 and P14 located 3D, 16D and 66D downstream of the vertical-downward elbow. Port P1, located 6D downstream of the inlet is chosen as reference. Hence, the local gauge pressure at all other port locations is obtained by:

$$P = P_1 - \rho g h - \Delta P_1 \tag{1}$$

Where, ' P_i ' represents the local gauge pressure at the i^{th} port location and 'Ii' represents the differential pressure between port P1 and the i^{th} port. Here, the term ΔP_{Ii} is measured by the differential pressure transducer. The differential pressure between two measurement locations can be represented as summation of frictional, minor and acceleration pressure drop. The pressure drop due to acceleration is very small and can be neglected. Hence, the theoretical expression for ΔP_{Ii} is given by Eq. 2.

$$\Delta P_{1i} = f\left(\frac{L}{D}\right) \frac{\rho v^2}{2} + \left(\sum k \frac{\rho v^2}{2}\right) \tag{2}$$

Where f, (L/D), ρ , v, and k denote the friction factor, development length, fluid density, fluid velocity and minor loss factor, respectively. In Eq. 2 the first term on the right hand side represents the frictional pressure drop and the second term represents the minor loss. The term due to minor loss is accounts for the vertical elbows along the test sections. The friction factor, f is obtained from the conventional Blasius correlation for turbulent flows [8]:

$$f = 0.316 \,\mathrm{Re}_{d}^{-1/4} \qquad 4000 < \mathrm{Re}_{d} < 10^{5} \tag{3}$$

The minor loss factor, k, for a 90° bend with single-phase water flow can be obtained from Ito [9] as:

$$k \approx 0.388\alpha \left(\frac{R}{d}\right)^{0.84} \operatorname{Re}_{d}^{-0.17} \tag{4}$$

Where,
$$\alpha = 0.95 + 4.42 \left(\frac{R}{d}\right)^{-1.96} \ge 1$$
 (5)

The single-phase liquid pressure drop across the 90-degree vertical elbows for the vertical upward-to-horizontal-to-vertical downward section is shown in Fig. 3a. It is found that the experimental data agree well with the theoretical predictions within $\pm 5\%$ difference. Fig. 3b shows the frictional and minor losses along the test section for the same flow conditions. The frictional pressure drop increases along the axial flow direction. The pressure drop across the vertical elbows is characterized by a steep change in pressure gradient, which is caused by the minor loss across the elbows.

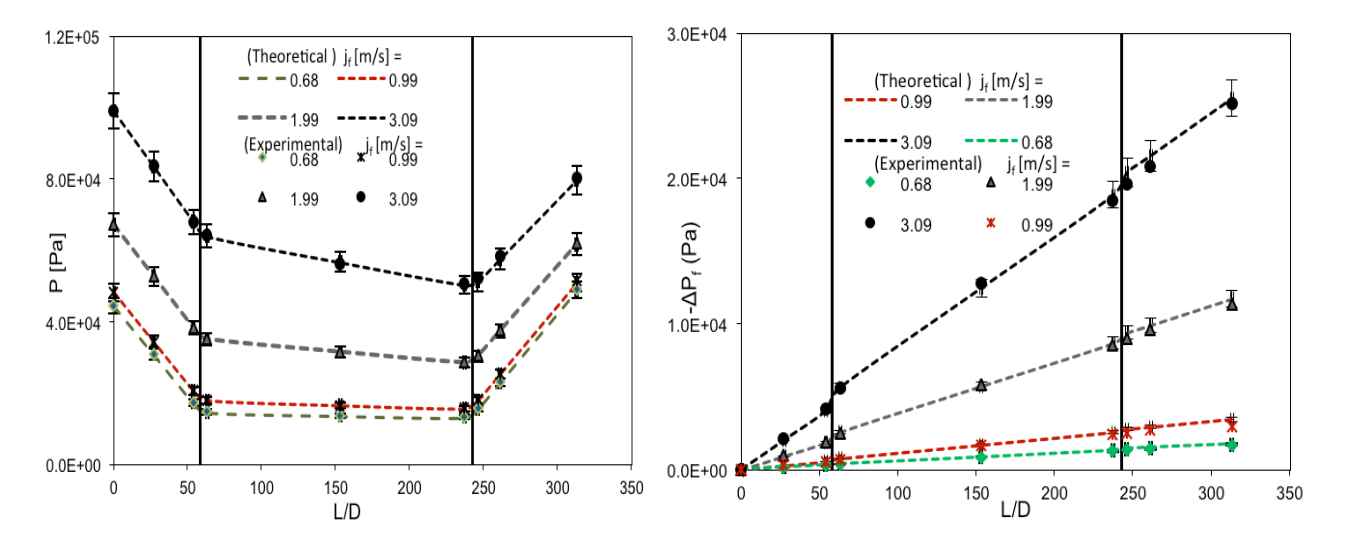


Figure 3 Comparison between theoretical prediction and experimental results for a) single-phase pressure drop b) frictional and minor loss along the test section.

2.2. Two-phase pressure

Two-phase pressure is measured at ten axial locations along the test section for six different flow conditions. The measurement locations correspond to ports P1, P2 and P3 located 6D, 33D and 60D

downstream of the inlet in the vertical-upward section. In the horizontal section the measurement locations correspond to ports P4, P5, P7 and P10 located 3D, 30D, 90D and 177D respectively, downstream of the vertical upward elbow. Measurement locations in the vertical-downward section correspond to ports P11, P12 and P14 located 2.5D, 18D and 60D respectively, downstream of the vertical downward elbow.

Figures 4a and 4b show the plot of local gauge pressure along the axial direction of the test section for flow conditions with constant liquid flow rates of 2.0 m/s and 3.0 m/s, respectively and increasing gas flow rates. In each figure the vertical lines represent the elbow location and hence subdivide the plot into vertical upward, horizontal and vertical downward section, respectively in the direction of increasing development length. In the vertical-upward section, the pressure decreases along the axial direction because of the frictional pressure drop and hydrostatic head loss. A steep pressure gradient observed in this section is due to the two-phase mixture hydrostatic head loss. The pressure drop between port P3 and P4 denotes the loss across the vertical-upward elbow and has contributions from minor loss, hydrostatic head and frictional pressure drop. The pressure gradient in the horizontal section is smaller compared to the vertical-upward because the pressure drop occurs only due to frictional losses. Similar to the vertical-upward elbow, the pressure drop across the vertical-downward elbow has contributions from minor loss, frictional loss and hydrostatic head. However, there is a gain in the pressure due to hydrostatic head and hence the net effect is an increase in the local gauge pressure. Similarly, in the vertical-downward section, the contributions arise from frictional pressure loss and hydrostatic head gain leading to an increase in the overall gauge pressure.

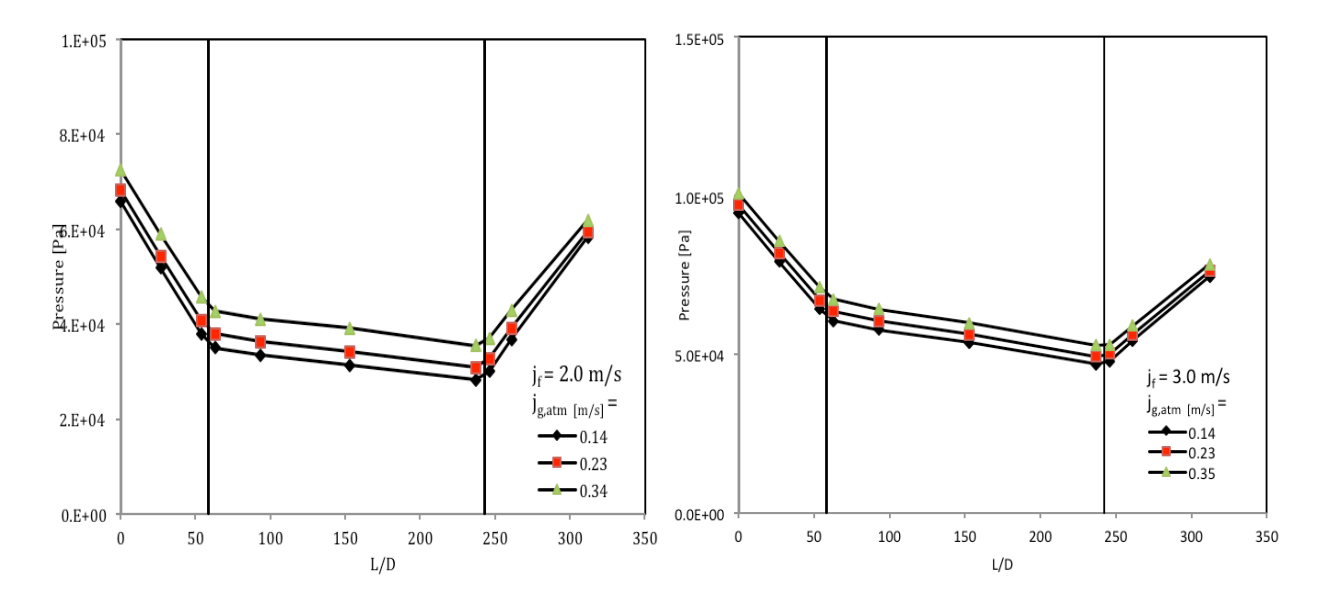


Figure 4 Two-phase pressure drop across 90-degree vertical elbows for flow conditions with a) constant liquid flow rate, $j_f = 2.0 \text{ m/s}$ and b) constant liquid flow rate, $j_f = 3.0 \text{ m/s}$.

In order to isolate the contributions due to frictional and minor loss along the test section, Fig. 5a shows the plot of pressure drop without the hydrostatic head along test section. Again the vertical lines represent the location of the elbows and differentiate vertical-upward, horizontal and vertical-downward section. As expected, the frictional pressure drop increases with the development length. Moreover, the elbow regions between ports P3 and P4 for the vertical-upward elbow and P10 and P11 for vertical-downward elbow are characterized by a steeper gradient due to the additional minor

loss occurring across the elbows. Figure 5b highlights the elbow region and shows the pressure drop across both vertical-upward and vertical-downward elbows.

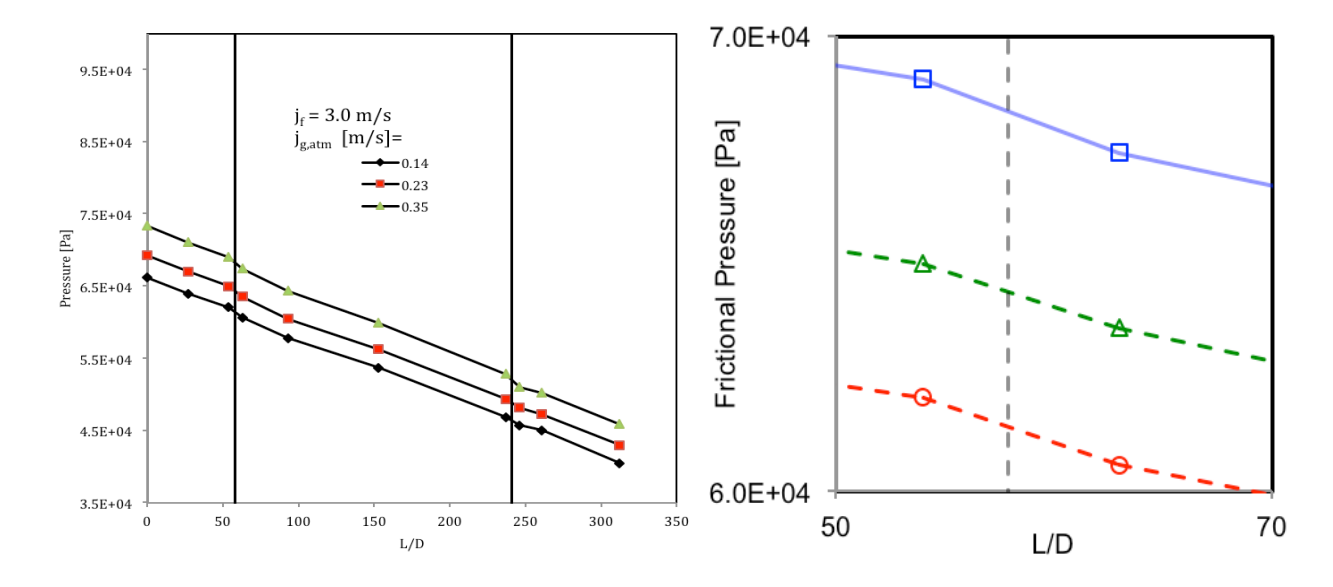


Figure 5 Two-phase pressure drop across 90-degree vertical elbows after removing the hydrostatic head for constant liquid flow rate, $j_f = 3.0$ m/s and increasing gas flow rates a) between ports P1 to P14 b) zoomed in view across the vertical upward elbow (P3-P4).

2.3. Two-phase pressure drop correlation

The conventional two-phase pressure drop correlation as postulated by Chisholm [10] and generally referred to as Lockhart & Martinelli correlation is given by Eq. 6. Here two-phase frictional pressure drop is written as the summation of each of the single-phase frictional pressure drop and a term representing the pressure drop due to the combination of the two fluids moving together simultaneously. Dividing Eq. 6 by the single-phase liquid frictional pressure drop leads to the expression in Eq. 7 in terms of two-phase multiplier (Φ^2) and Lockhart & Martinelli parameter X. In Eq. 7 C is the constant whose numerical value is found to be 20 for horizontal two-phase flow [10].

$$\left(\frac{dp}{dz}\right)_F^{2\phi} = \left(\frac{dp}{dz}\right)_F^f + \left(\frac{dp}{dz}\right)_F^g + C\left[\left(\frac{dp}{dz}\right)_F^f \left(\frac{dp}{dz}\right)_F^g\right]^{1/2} \tag{6}$$

$$\phi^2 = 1 + \frac{1}{X^2} + \frac{C}{X} \tag{7}$$

Figures 6a and 6b show the comparison of two-phase pressure in the vertical-upward section and vertical-downward section, respectively with Lockhart-Martinelli prediction. It should be noted that the numerical value of C varies depending on the flow configuration and is found to be 40 for the vertical-upward section and 10 for vertical-downward section. This demonstrates that the value of C not only depends on the flow configuration but also on flow direction. It should be noted that the best fit in the vertical downward flow is obtained for a value of C = 10, which is contrary to the expected value of C = 40. Figures 7a and 7b shows the prediction of two-phase pressure in the horizontal section and overall pressure drop, respectively. Moreover, the overall pressure drop between ports P1 and P10

can be best predicted with a value of C = 30. Interestingly, the value of C for the vertical-to-horizontal configuration is an average of the value of C for the vertical section and the horizontal section.

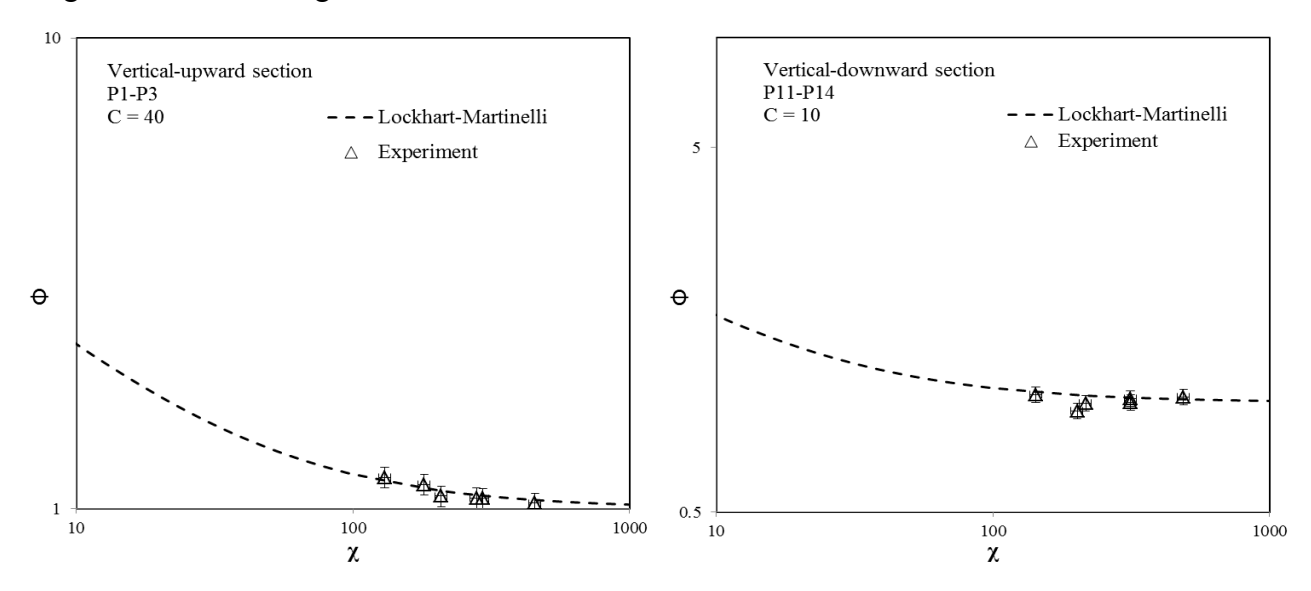


Figure 6 Comparison of two-phase pressure drop with Lockhart-Martinelli prediction along a) vertical-upward section b) vertical-downward section.

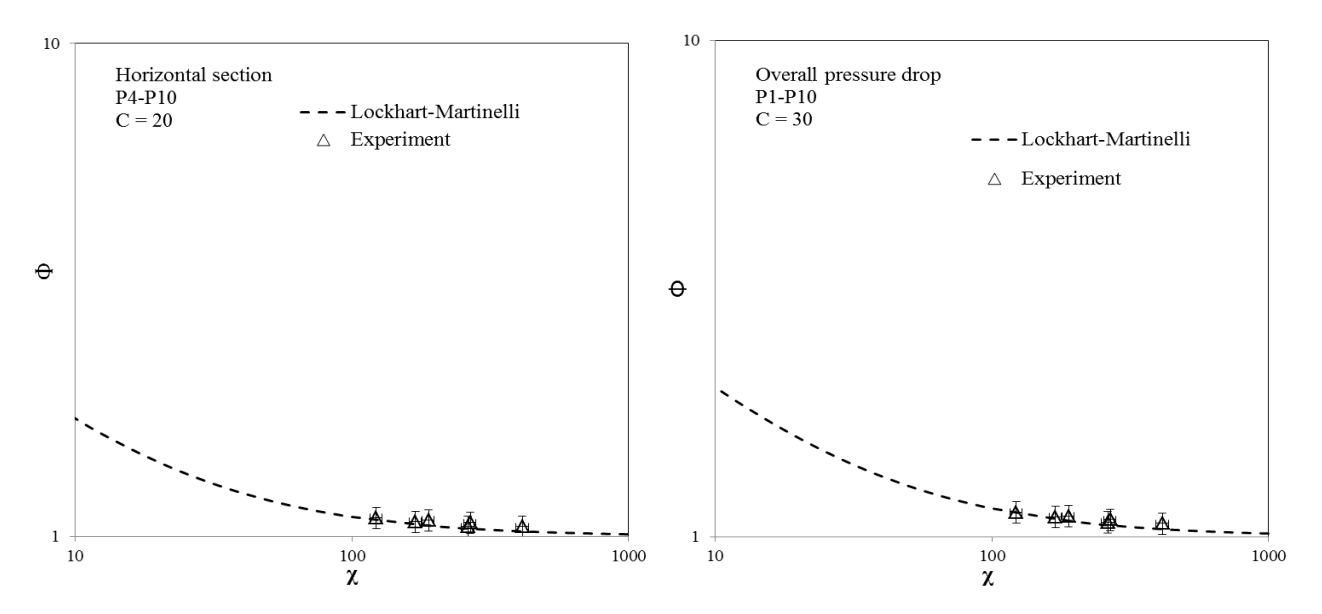


Figure 7 Comparison of two-phase pressure drop with Lockhart-Martinelli prediction along a) horizontal section and b) vertical upward-to-horizontal section.

Prediction of two-phase pressure drop along straight pipes as well as across the flow restrictions is one of the challenging problems with several applications. Most of the efforts in past were directed towards predicting two-phase pressure drop in straight pipe sections. Kim et. al. [7] presented a model similar to the Lockhart and Martinelli correlation to predict pressure drop across horizontal elbows. A simple model based on the Lockhart and Martinelli correlation is proposed here to predict the pressure drop across the elbows. Total two-phase pressure drop across the elbow is divided into contributions due to the frictional pressure drop and the minor loss as shown in Eq. 8. The two-phase frictional pressure drop is expressed in terms of frictional pressure drop due each of the single-phase components

and a combination of the two-phases as shown in Eq. 9. Division of Eq. 9 by single-phase liquid pressure drop yields a familiar equation in terms of two-phase flow multiplier and Lockhart-Martinelli parameter as well as an additional term for minor loss across the elbow as shown in Eq. 10.

$$\left(\frac{dp}{dz}\right)_{Total}^{2\phi} = \left(\frac{dp}{dz}\right)_{F}^{2\phi} + \left(\frac{dp}{dz}\right)_{M}^{2\phi} \tag{8}$$

$$\left(\frac{dp}{dz}\right)_{Total}^{2\phi} = \left(\frac{dp}{dz}\right)_{F}^{f} + \left(\frac{dp}{dz}\right)_{F}^{g} + C\left[\left(\frac{dp}{dz}\right)_{F}^{f}\left(\frac{dp}{dz}\right)_{F}^{g}\right]^{1/2} + \left(\frac{dp}{dz}\right)_{M}^{2\phi} \tag{9}$$

$$\phi^2 = 1 + \frac{1}{X^2} + \frac{C}{X} + \frac{1}{X_M^2} \tag{10}$$

Where,
$$\phi^2 = \frac{\left(\frac{dp}{dz}\right)_{Total}^{2\phi}}{\left(\frac{dp}{dz}\right)_F^f}$$
 and $X^2 = \frac{\left(\frac{dp}{dz}\right)_F^f}{\left(\frac{dp}{dz}\right)_F^g}$ and $X_M^2 = \frac{\left(\frac{dp}{dz}\right)_F^f}{\left(\frac{dp}{dz}\right)_M^2}$

The frictional pressure drop for single-phase fluid can be obtained using the Fanning equation as shown in eq. 4.

$$\left(\frac{dp}{dz}\right)_F^i = \frac{2f}{D}\rho_i j_i^2 \tag{11}$$

Where, the friction factor
$$f$$
 is given by: $f = m \operatorname{Re}^{-n}$ (12)

In the current formulation, the minor loss across the elbow is formulated similar to the minor loss in single-phase flow using the minor loss coefficient, k as shown in Eq. 3-14. However, the fluid properties are replaced with the mixture properties and fluid velocity is replaced with the total superficial velocity.

$$\left(\frac{dp}{dz}\right)_{M}^{2\phi} = \frac{k}{L} \frac{\rho_{m} j^{2}}{2} \tag{13}$$

Where, ρ_m is the mixture density and j is the total superficial velocity as shown below

$$\rho_m = \alpha \rho_g + (1 - \alpha)\rho_f \qquad \text{and} \qquad j = j_g + j_f$$
 (14)

The above correlation is developed for pressure drop across the elbows. Hence, Fig. 8a shows the pressure drop predictions between ports P3 and P4, i.e. across the vertical-upward elbow. Two-phase pressure measurements across the elbow from the experiment are plotted against the model predictions. The best fit for the experimental data is obtained at C = 80 and k = 0.04 and the absolute average error is found to be 3.8%. Similarly, for the pressure drop across vertical-downward elbow the best fit is obtained at C = 80 and C

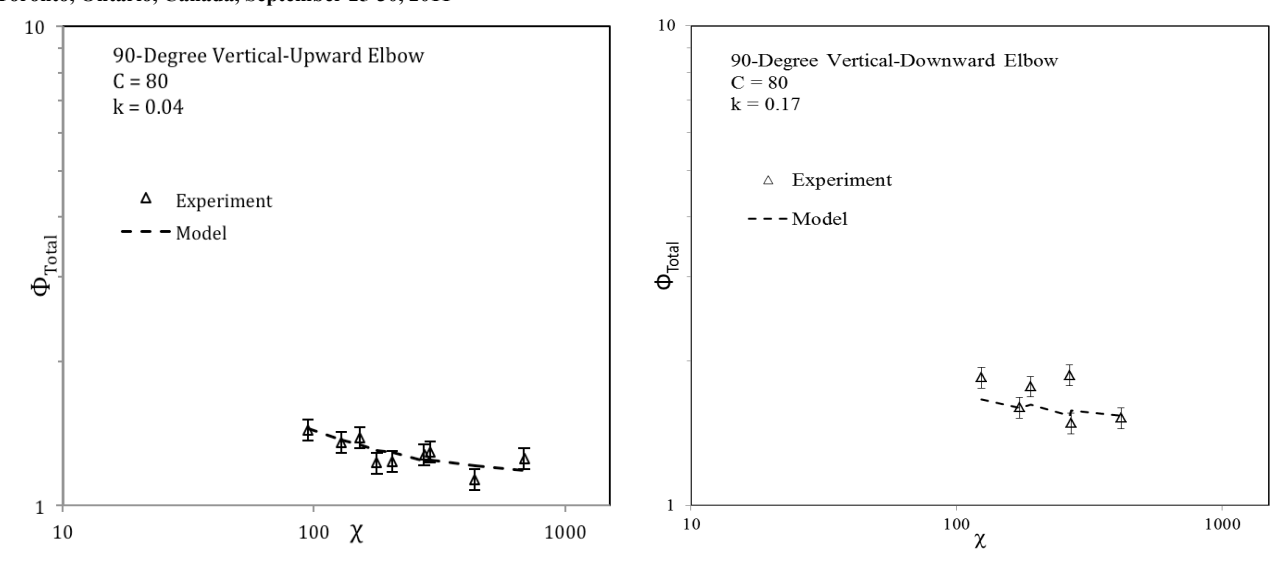


Figure 8 Comparison of two-phase pressure drop with new correlation predictions across a) 90-degree vertical-upward elbow b) 90-degree vertical downward elbow.

The new correlation is also used to predict the pressure drop data obtained from previous experiments [7] across 90-degree and 45-degree horizontal elbows in bubbly two-phase flow conditions. Figure 9a and 9b show the comparison between the new correlation and the experimental data for 90-degree and 45-degree horizontal elbows, respectively. The best agreement is obtained for C = 80 for both the elbows and k = 0.61 and 0.35 for 90-degree and 45-degree elbow, respectively. The absolute average error is found to be 2.08% and 1.35% for 90-degree and 45-degree horizontal elbows, respectively.

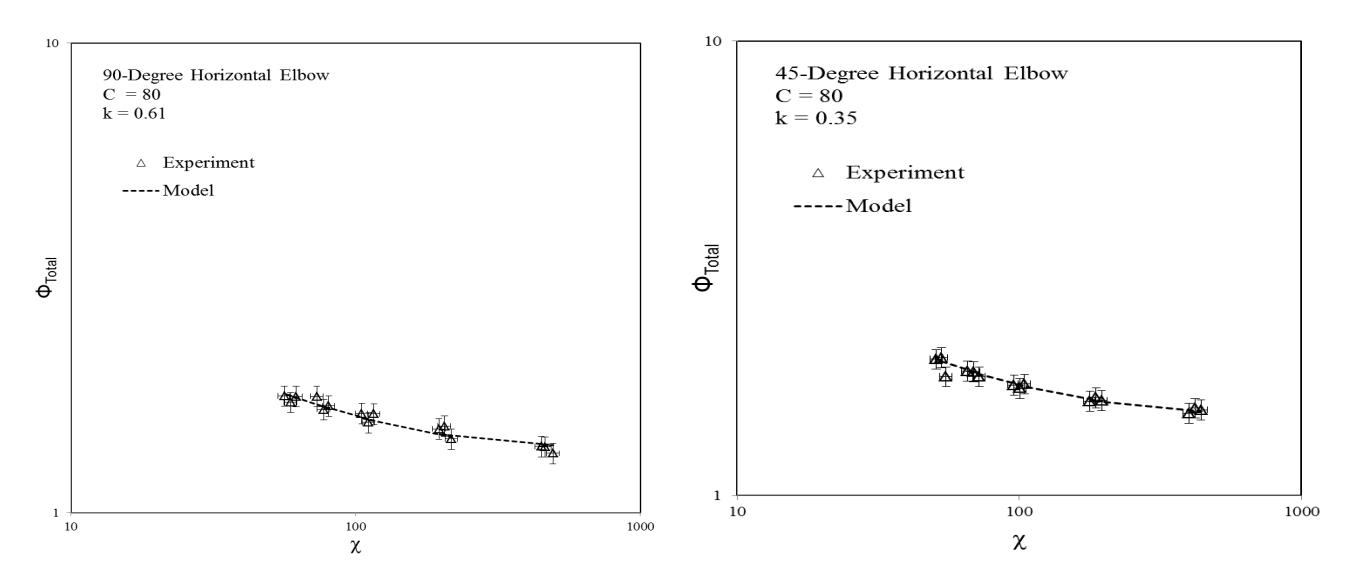


Figure 9 Comparison of two-phase pressure drop with new correlation predictions across a) 90-degree horizontal elbow b) 45-degree horizontal elbow.

It is observed that in all the above cases, a good agreement with the experiment is obtained by keeping a constant value of C = 80 and varying the minor loss coefficient, k. Furthermore, the value of C = 80 is higher across the elbows compared to the value of C = 20 for straight pipes in the conventional Lockhart-Martinelli correlation. It is speculated that the higher value of C is because of the following factors:

- Buoyancy effect due to change in the flow orientation.
- Irreversible work performed due to bubble interaction promoted by the elbow and interaction between the two phases as they move across the elbow.
- Pressure drop due to distribution of the dispersed phase (bubbles tend to follow the secondary flow streamlines).

2. Flow Regime Identification

Extensive flow visualization is performed at various axial locations along the test section in order to study the geometric effects of 90-degree vertical elbows and flow configurations on two-phase flow regime transition. A comprehensive set of flow conditions chosen to span bubbly and slug flow regime in the vertical upward section are investigated at different axial locations along the test section. The measurement locations include: port P3 located in the vertical upward section at 60D downstream of the inlet, ports P4, P7, P9 and P10 located in the horizontal section at 3D, 90D, 147D and 177D downstream of the vertical upward elbow, respectively and ports P11 and P14 located in the vertical downward section at 3D and 66D downstream of the vertical downward elbow, respectively. Figure 10 shows a typical high-speed image highlighting the effect of the 90-degree vertical upward elbow on two-phase flow structure. As evident from the image, a cap-bubble in the vertical section gets broken into smaller bubbles as it passes through the elbow region. Further downstream of the elbow, these smaller bubbles migrate towards the top wall of the pipe and coalesce to form a plug bubble. This shows that in general, the elbow causes break-up of the large bubbles and hence immediately downstream of the elbow we can expect the flow regimes to shift towards bubbly flow.

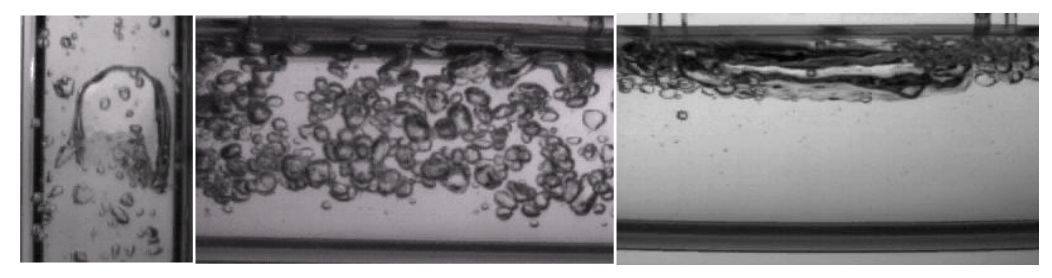


Figure 10 High-speed images obtained at 2000 frames per second, showing the development of twophase flow structure across the vertical-upward elbow.

Experimental results from flow visualization at port P3 (60D downstream of the injection) in the vertical-upward section are compared with the flow regime transition boundaries suggested by Mishima and Ishii [11]. The flow regime transition boundaries obtained from the experiment are found to be in good agreement with the conventional theoretical flow regime transition boundaries. This shows, as expected, that the elbow has negligible effect on the flow regime transition at upstream locations.

2.4.1 Horizontal section

The flow visualization results in the horizontal section are compared with the flow regime maps suggested by Mandhane et. al. [12]. Figure 11a shows the modified flow regime map at port P4, located at 3D downstream of the vertical elbow. The solid lines represent the modified flow regime boundaries and the dashed lines represent the conventional flow regime boundaries. As mentioned earlier, the elbow causes the breakup of large bubbles. Hence, the bubbly flow regime exists even at lower liquid flow rates and extends into the conventional plug flow regime. It is speculated that the secondary flow in the elbow causes bubble disintegration. Moreover, the elbow generated

turbulence causes the slug flow regime to occurs at lower gas flow rates and extend into the conventional plug flow regime. It is important to note that in the nuclear reactors the development length downstream of the flow restrictions is very small and hence modified flow regime maps are required to accurately identify the flow pattern.

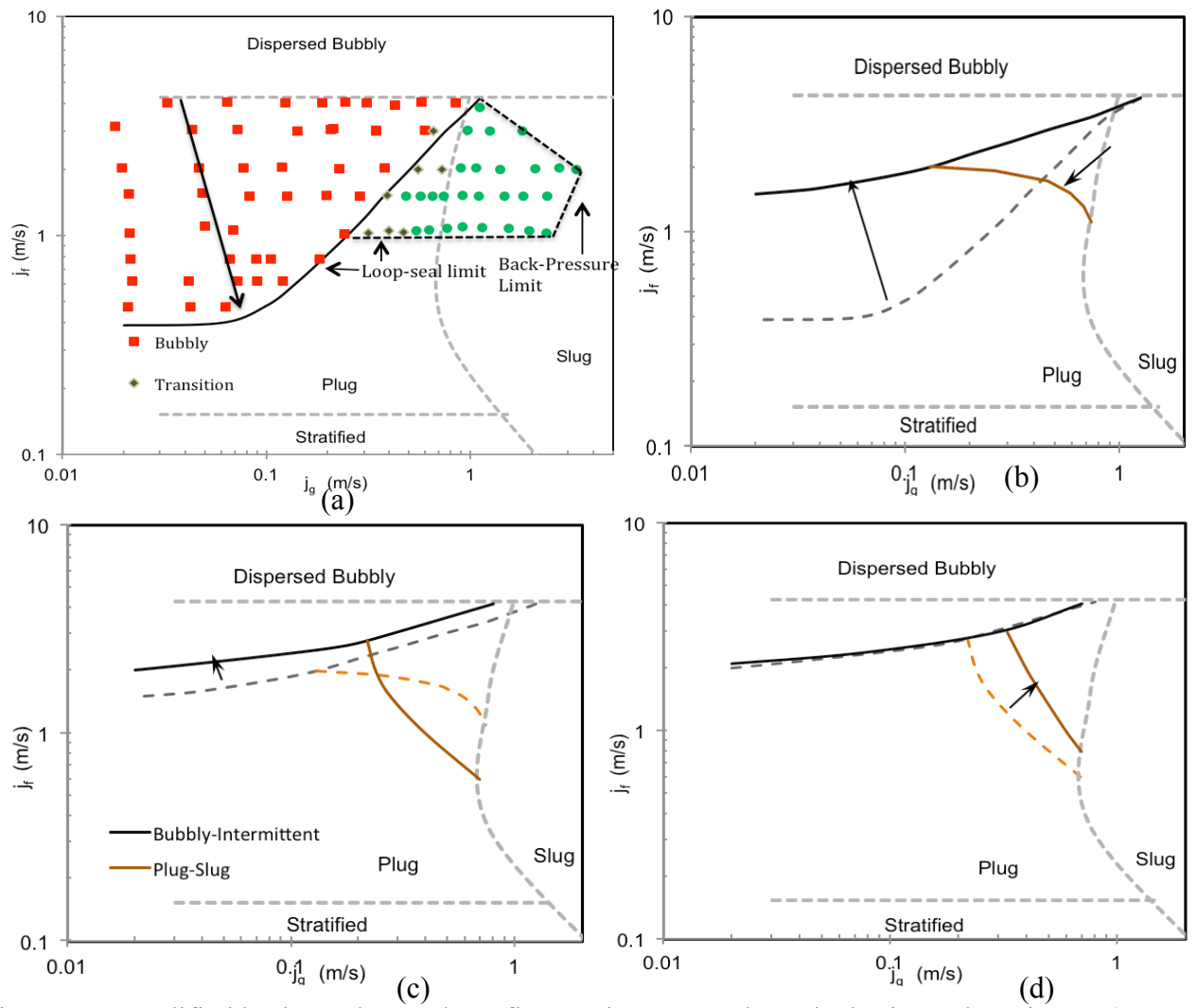


Figure 11 Modified horizontal two-phase flow regime maps along the horizontal section at a) port P4, b) port P7, c) port P9, and d) port P10.

Figure 11b shows the modified flow regime map at port P7, located 90D downstream of the vertical elbow. The two-phase flow becomes more developed by this measurement location. The bubbles tend to rise towards the upper pipe wall and coalesce in the process. This causes the bubbly flow regime to move towards the higher liquid flow rates and conventional flow regime boundary. Moreover, the slug flow boundary recedes towards the conventional boundary and the plug flow regime starts to appear again. The effect of development length on the flow regime transition boundaries is shown in Figs. 11c and 11d corresponding to the modified flow regime maps at P9 and P10, located 147D and 177D downstream of the vertical elbow. It is observed that the modified flow regime boundaries migrate towards the conventional flow regime boundaries. However, significant elbow effect is present even at a development length of 177D. It is assumed that the modified flow regime boundaries would converge with the conventional flow regime boundaries

further downstream. It also suggests that horizontal two-phase flow requires more than 180D to fully develop.

2.4.2 Vertical-downward section

As mentioned earlier, flow visualization is performed at two axial locations in the vertical downward section. Flow visualization at port P11 (L/D = 2.5) shows the effect of the vertical downward elbow on flow regime transition and at port P14 (L/D = 66) demonstrates the effect of development length in the vertical downward two-phase flow. The flow visualization results are then compared with flow regime map for vertical downward flow obtained by Kim et. al. [13]. Figure 12a shows the vertical downward flow regime map at port P11. It is observed that there is a prominent transition region between bubbly and slug flow regime. Within this region elongated bubbles with shapes similar to Taylor bubble are observed, however, the bubbles do not occupy the entire pipe cross-section. Moreover, slug flow regime occurs in the region occupied by churnturbulent flow in conventional flow regime map. This happens because compared to conventional two-phase injector, vertical downward elbow serves as injection in the current study. Moreover, this shows the effect of the elbow in vertical downward flow regime transition. Figure 12b shows the flow regime map for vertical-downward two-phase flow at port P14 located 66D downstream of the vertical-downward elbow. The effect of development length can clearly be seen as the flow regime transition boundaries approach the conventional boundaries. A major difference from the conventional flow regime map is lack of churn turbulent flow and presence of a prominent transition to slug region in the modified flow regime map. This difference arises due to different two-phase flow injection and method of flow regime identification.

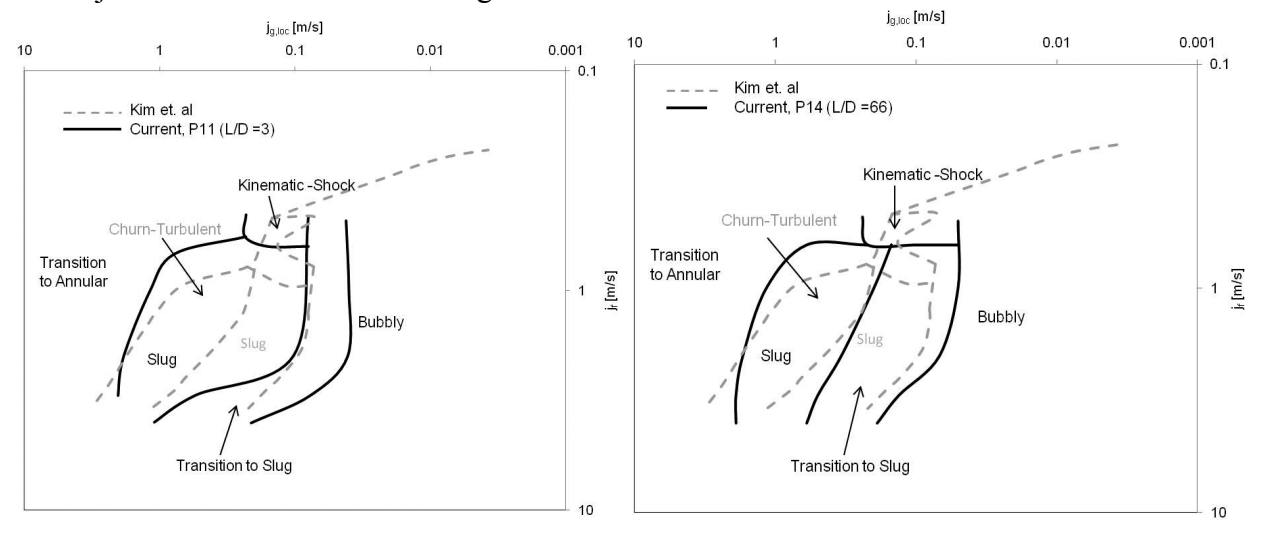


Figure 12 Modified horizontal two-phase flow regime map for vertical-downward two-phase flow at a) port P11 and b) port P14.

3. Conclusion

Geometric effects of 90-degree vertical elbows on pressure drop and two-phase flow regime transition are shown. It is shown that the elbows create an additional pressure drop in the test section due to the minor losses. A preliminary correlation analogous to the Lockhart-Martinelli correlation is developed to predict pressure drop across the elbows. The new correlation predicts the data well within an average error of $\pm 5\%$. The geometric effects of 90-degree vertical elbows on two-phase

flow structure are clearly demonstrated in flow regime transition. Flow regime identification is performed via flow visualization by employing a high-speed camera. It is found that the 90-degree vertical elbows have significant impact on the flow regime transition in the corresponding downstream sections. The elbows, in general, cause the bubbles to break-up. As such modified flow regime maps are obtained for both horizontal and vertical-downward section. Furthermore, it is found that horizontal two-phase flow is not fully developed even at approximately 180 pipe diameters downstream of the vertical-upward elbow.

Acknowledgements

This research is supported by the U.S DOE through DOE NEER Program.

4. References

- [1] M. E. Salcudean, D. C. Groeneveld and L. K. H. Leung, "Effect of flow obstruction geometry on pressure drop in air-water flow", Int. J. Heat and Mass Transfer, Vol. 25, No. 5, 1983, pp. 723-737.
- [2] M. E. Salcudean, and L. K. H. Leung, "Two-phase pressure drop through obstructions", Nuclear Engineering Design, Vol. 105, 1988, pp. 349-361.
- [3] C. Wang, I. Y. Chen, Y. Yang and R. Hu, "Influence of horizontal return bend on the two-phase flow pattern in small diameter tubes", Experimental Thermal and Fluid Sci., Vol. 28, 2004, pp. 145-152.
- [4] S. T. Hwang, H. M. Soliman, and R. T. Lahey, "Phase separation in dividing two-phase flows", Int. J. Multiphase Flow, Vol. 14, No. 4, 1988, pp. 439-458.
- [5] J. M. Chenoweth and M. W. Martin, "Turbulent two-phase flow", Pet. Ref., Vol. 34, No. 10, 1955, pp. 151-155.
- [6] P. L. Spedding, and E. Benard, "Gas-liquid two phase flow through a vertical 90° bend", Experimental Thermal and Fluid Sci., Vol. 31, 2007, pp. 761-769.
- [7] S. Kim, G. Kojasoy, T. Guo., "Two-phase minor loss in horizontal bubbly flow with elbows: 45 degree and 90 degree elbows", Nuclear Engineering Design, Vol. 240, 2010, pp. 284-289.
- [8] H. Blasius, "Das Ähnlichkeitsgesetz bei reibungsyorgängen in flüssigkeiten", Ver. Dtsch. Ing. Forschungsh", 1913, pp. 131.
- [9] H. Ito, "Flow in curved pipes", JSME International Journal, Vol. 30, 1987, pp. 543-552.
- [10] D. A. Chisholm, "Theoretical basis for the Lockhart-Martinelli correlation for two-phase flow", Int. J. Heat Mass Transfer, Vol. 10, 1967, pp. 1767-1768.
- [11] K. Mishima, and M. Ishii, "Flow regime transition criteria for upward two-phase flow in vertical tubes", Int. J. Heat and Mass Transfer, Vol. 25, No. 5, 1983, pp. 723-737.
- [12] J. M. Mandhane, G. A. Gregory and K. Aziz, "A flow pattern map for gas-liquid flow in horizontal pipes", Int. J. of Multiphase Flow, Vol. 1, 1974, pp. 537-553.
- [13] S. Kim, S. S. Paranjape, M. Ishii and J. Kelly "Interfacial structures and regime transition in co-current downward bubbly flow", J. Fluids Eng., Vol. 126, 2004, pp. 528-538.